## DEVELOPMENT OF ESTIMATION METHOD OF VEHICLE'S EMERGENCY HANDLING

**Kenichi Kitahama**
**Masami Aga**
**Takashi Yonekawa**
Toyota Motor Corporation, Japan

Paper Number 542

### ABSTRACT

First, for evaluating vehicles' emergency handling performance in real world, we set several course patterns of closed-loop test (task performance test) similar to occurring patterns of real accidents, and measure the vehicles' maximum entering velocity of each course.

Second, we normalize the velocity by each vehicle's basic dimensions (mass, height of center of gravity, tread etc.), which enable us to compare the tire and suspension performance.

Last, we produce an estimation method of the results of the closed-loop tests, using a vehicle's design parameters, which include basic dimensions, suspension and tire. We consider that this estimation method can reduce the time for developing cars.

### INTRODUCTION

A vehicle's handling near the grip limit of the tires and the operating limit of the driver (i.e., its emergency handling) is an important element of the vehicle's basic performance. In order to evaluate emergency handling, the authors established course pattern models based on the patterns that occur in actual accidents and measured the maximum entering velocity at which vehicles can traverse each course.

In the study reported here, the authors devised a method of comparing the suspension specifications and the tire characteristics on the basis of the measured maximum entering velocity while excluding the influence of the basic vehicle specifications (those that physically determine the vehicle's basic handling and that can not be largely changed after the planning stage).

Also, to shorten the development period, the authors developed a technique for estimating the maximum entering velocity for the courses on the basis of the basic vehicle specifications, the suspension specifications, and the tire characteristics. This made it possible to propose specifications that would achieve the target velocity at the design stage.

### TESTING METHOD

#### Test Course

The left side of Figure 1 shows the classes of major accidents that actually occur when the driver becomes unable to control the vehicle. The course patterns on the right side of Figure 1 were determined by modeling the patterns of these accidents. In total, nine patterns were established taking dry and wet road surfaces into account.

The maximum entering velocity at which a vehicle can traverse a course without going outside the bounds of the course is thought to be one indicator of how high the emergency handling limit is. The driver is allowed to make the maximum effort at corrective steering at this time. Also, a maximum entering velocity was used at which the stopping distance would be 50 meters for either straight line braking or braking while cornering.

#### Method of excluding basic specifications

To compare the emergency handling of a vehicle with different basic specifications, a method was devised that excludes the effects of the basic specifications and compares only the tires, suspension, and braking performance.

Figure 2 is based on the assumed maximum entering velocities of multiple vehicles on a given course. The horizontal axis is set to either $m/(A_{x0})^2$ (for straight line braking) or $m/(A_{y0})^2$ (for courses other than straight line braking). Here, m is the vehicle mass, $A_{x0}$ is half the wheel base divided by the height of the center of gravity, and $A_{y0}$ is half the tread width divided by the height of the center of gravity. The horizontal axis thus expresses the basic specifications of the vehicle.

In this case, the maximum acceleration in the longitudinal and lateral directions is the dominant vehicle characteristic affecting emergency handling, and in dynamic calculation, $m/(A_{x0})^2$ and $m/(A_{y0})^2$ become linear functions (with negative slope). (Refer to equation (2) in section Method of estimating cornering limit) Therefore, the performance when the tire and suspension characteristics are average, as calculated by equation (2), is shown in Figure 2 as a bold line sloping down to the right. The difference $\Delta V$ from the bold line is thought to be the maximum entering velocity excluding the effects of the basic specifications, which are difficult to change after the planning stage, and to express only the tires, suspension, and braking performance.

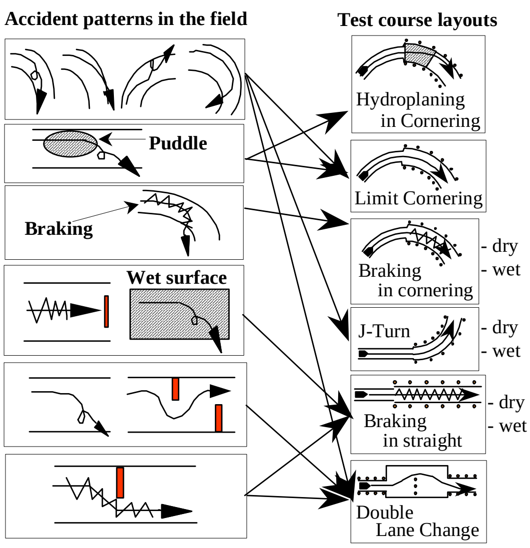


**Figure 1. The course layouts**

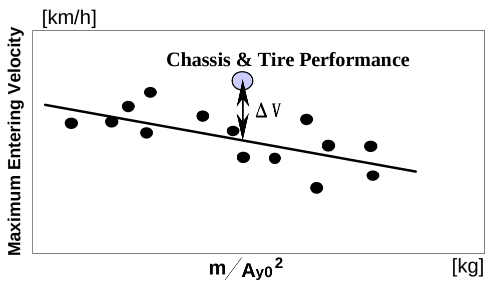


**Figure 2. The elimination of the basic dimensions**

## PERFORMANCE ESTIMATION

A technique was devised for estimating the maximum entering velocity for each course on the basis of the basic specifications, tire specifications, and suspension specifications. Figure 3 shows the relationship among the course layouts (on the left), the vehicle dynamics of interest (in the middle), and the parameters that are incorporated into the estimation calculations (in the right).

For example, for straight line braking, the focus is on the maximum acceleration in the longitudinal direction, which is calculated from the basic specifications and the tire characteristics. This section describes the estimation calculation techniques using the cornering limit, braking while cornering, double lane changing, and hydroplaning while cornering as examples.

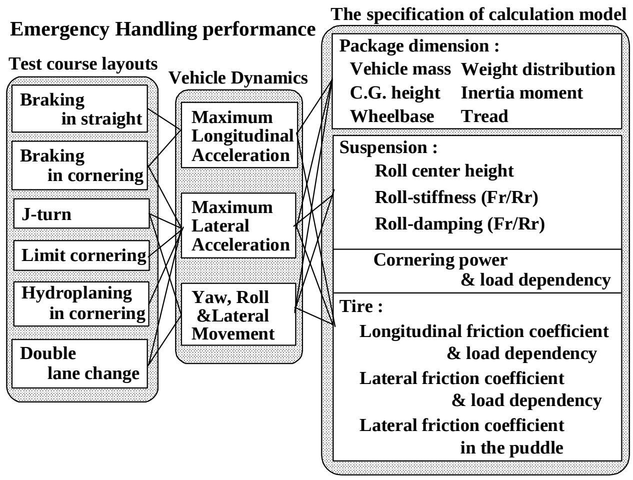


**Figure 3. The relationship of test task and calculation model**

## Method of estimating cornering limit

The maximum entering velocity in the cornering limit test ($u_{max}$) is determined by the maximum lateral acceleration that can be generated by the vehicle. If the respective estimated maximum lateral accelerations generated by the front and rear wheels are expressed in the form $A_{yi}$ (where i is 1 for the front wheels and 2 for the rear wheels), the maximum lateral acceleration used to determine the maximum entering velocity in the cornering limit test is equal to the smaller $A_y$ of those two values. This is expressed by the following equation:

$$u_{max} = \sqrt{A_y R} \qquad (A_y = min[A_{y1}, A_{y2}]) \qquad (1)$$

In this equation, R is the cornering radius. That is to say, if $A_{yi}$ can be calculated, then $u_{max}$ can be estimated using equation (2).

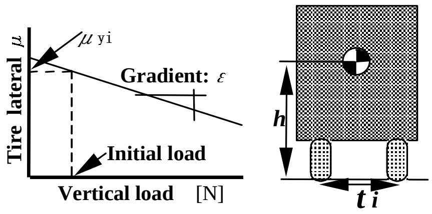


**Figure 4. Tire and Vehicle calculation model**

The relationship between the lateral friction coefficient $\mu$ and vertical load of the tires is shown on the left side of Figure 4 by a model that approximates a linear function. The vehicle is shown on the right side of Figure 4 by an integrated sprung/unsprung rigid body model (front/rear half model). If these two models are transformed into equation form so that the sum of the side forces of the left and right wheels derived as a function of $A_{yi}$ is equal to the operating centrifugal force, then $A_{yi}$ can be formulated approximately by the following equation:

$$A_{yi} = \left(1 - \frac{1}{2}\mu_{yi}\frac{D_{ri}^2}{D_{wi}}\frac{m}{A_{y0}^2}\varepsilon g\right)\mu_{yi} g \qquad (2)$$

i=1 : Fr, i=2 : Rr,
$\mu_{yi}$: Lateral tire $\mu$ at initial load
$\varepsilon$ : Load dependency of Tire lateral
$D_{wi}$: Weight distribution(Fr,Rr)
$D_{ri}$: Stiffness distribution of roll (Fr,Rr)
$m$: Vehicle mass
$g$: Gravity
$t_i$: Tread
$h$: C.G. height
$A_{y0}$: $(= t_i/2/h)$

$A_{yi}$ can be calculated by substituting the specification values into equation (2), and $u_{max}$ can be estimated using equation (1).

### Method of estimating braking while cornering

The braking while cornering maneuver measures the entering velocity for which the stopping distance is 50 meters when full braking is used (with ABS operating) as the vehicle follows a circular path with a radius of 100 meters.

The maximum lateral acceleration $A_{xmax}$ is also calculated in the same way using the technique described in section Method of estimating cornering limit. And as shown in Figure 5, the oval of friction described by $A_{xmax}$ and $A_{ymax}$ that results from the effect of ABS is utilized to the maximum during braking while cornering. That is to say, the lateral acceleration at the perimeter of the oval of friction is postulated as the lateral acceleration generated by the front and rear wheels respectively.

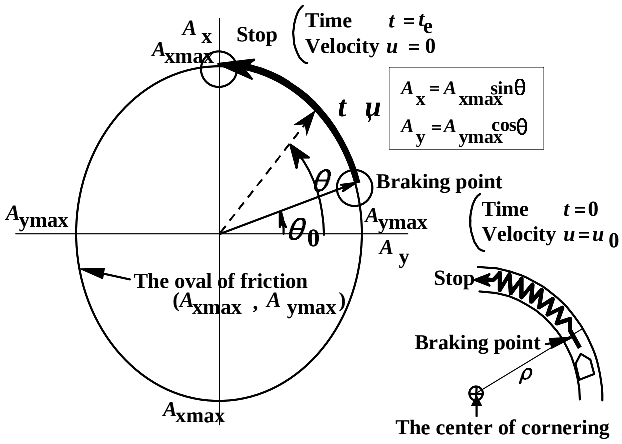


**Figure 5. The calculation of braking in the cornering**

Braking starts at the point on the perimeter of the oval that corresponds to angle $\theta_0$ in Figure 5. Also, if the lateral acceleration at the instant the vehicle stops is posited to be zero, braking can be thought to end at the apex of the oval of friction. Friction during braking is expressed by equation (3).

$$u=\sqrt{\rho g A_{y\max}\cos\theta} \qquad (3)$$

If both sides of this equation are differentiated by time t, the result is equation (4).

$$\frac{du}{dt} = -\frac{\sqrt{\rho g A_{y\max}}\,\sin\theta}{2\sqrt{\cos\theta}}\;\frac{d\theta}{dt} \qquad (4)$$

On the other hand, because equation (5) also holds true, equations (4) and (5) can be reconciled into equation (6).

$$\frac{du}{dt} = A_{x\max}\sin\theta \qquad (5)$$

$$dt = -\frac{\sqrt{\rho g A_{y\max}}}{2A_{x\max}\, g\sqrt{\cos\theta}}\, d\theta \qquad (6)$$

Using equations (3) and (6), the stopping distance L can be written by the following equation:

$$L=\int_0^{t_e} u\,dt = \frac{\rho g A_{\mathrm{ymax}}}{2A_{\mathrm{xmax}}}\int_{\theta_0}^{\frac{\pi}{2}} d\theta = \frac{\rho g A_{\mathrm{ymax}}}{2A_{\mathrm{xmax}}}\left(\frac{\pi}{2}-\theta_0\right) \qquad (7)$$

On the other hand, because equation (8) also holds true.

$$u_0=\sqrt{\rho g A_{y\max}\cos\theta_0} \qquad (8)$$

The entering velocity that determines the stopping distance L can be expressed by equation (9).

$$u_0 = \sqrt{A_{ymax}\rho g \sin\left(\frac{2L\, A_{xmax}}{\rho\, A_{ymax}}\right)} \qquad (9)$$

## Method of estimating double lane change

### (1) Course trajectory

A trajectory was posited that consists of two single lane changes in sequence (an avoidance change and a return change), as shown in Figure 6. It is generally known that the trajectory of a single lane change is expressed as a ramp wave plus a sine wave.(1) Therefore, with the four points marked by stars, as shown in Figure 6, posited as restraining points (on the assumption that the vehicle passes through shaving the course), the trajectories of the ramp wave and the sine wave were derived according to the width of each vehicle. The lengths of the avoidance lane change and the return lane change, derived in this way, were almost equal.

**assumption: Composed 2 single lane change.**

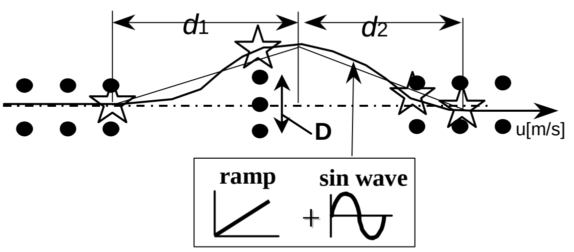


**Calculation of the trajectory for passing 4 ☆ .**

**Required lateral acc.:** $A_{ymax0} \cong \pi \dfrac{D+W}{\left((d_1+d_2)/2\right)^2} u^2$
$W$ :vehicle width

**Figure 6. The trajectory for passing in double lane change**

### (2) Dynamic maximum lateral acceleration of front and rear wheels

A double lane change provides dynamic steering inputs. For that reason, the dynamic maximum lateral acceleration $A_{yi}^*$ is different from the static steering input $A_{yi}$ derived in section Method of estimating cornering limit and becomes a function of the steering frequency.(2) The upper half of Figure 7 is an example of a linear model of a vehicle (with 3 degrees of freedom: yaw, body slip angle, and roll angle)(3) in which the value of $A_{yi}^*$ is calculated with cyclic steering as a given. The dynamic maximum lateral acceleration that a vehicle actually generates is the smaller of the two $A_{yi}^*$ values.

Because the lengths of the avoidance lane change and the return lane change are almost equal, if it is assumed that the vehicle is driven at a fixed steering frequency, the steering frequency is determined by the length of each lane change and the vehicle velocity, so the horizontal axis can be converted from steering frequency to vehicle velocity, as shown in the lower half of Figure7.

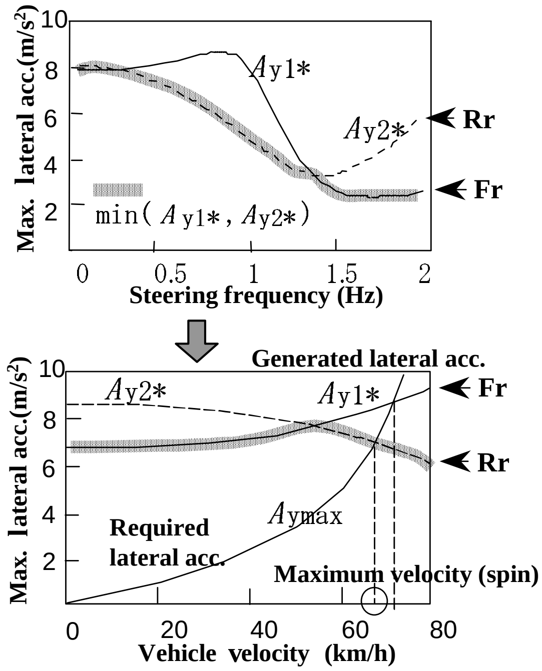


**Figure 7. The calculation of Max. lateral acc. and Max. velocity**

### (3) Estimation of vehicle velocity

The lower half of Figure 7 also shows the estimated maximum lateral acceleration $A_{ymax}$ that can be generated when the vehicle follows the trajectory that was derived in section Method of estimating double lane change, (1).

The x coordinates at the intersections of $A_{yi}$ and $A_{ymax}$ were defined as $u_{imax}$, with the smaller of the two $u_{imax}$ values defined as the maximum entering velocity $u_{max}$. When $u_{max}$ is $u_{1max}$, the graph shows the lateral slip of the front wheels (plowing), and when $u_{max}$ is $u_{2max}$, the graph shows the lateral slip of the rear wheels (spin). (Figure 7 is the graph for spin.)

## Method of estimating hydroplaning while cornering

This maneuver is used to evaluate the vehicle's stability versus external disturbances (in this case, the changes in the road surface coefficient of friction $\mu$. when the vehicle enters a puddle) during cornering. The actual movements are complex, so the vehicle is expressed as mass points, as shown in Figure 8, and attention was focused only on the deflection of the travel trajectory resulting from the changes in the road surface $\mu$.

During the maneuver, velocity $u_0$ is assumed to be fixed. While the vehicle is passing through the puddle, the lateral G force that can be generated decreases, causing the cornering radius $\rho_1$ to become larger. After the vehicle leaves the puddle, it is assumed that it corners with the maximum lateral G force. If the velocity is increased, the vehicle makes contact with the outer side of the course at point A in Figure 8, and the velocity at which it does so is calculated as the maximum entering velocity.

On the other hand, the results of measurements made using quite a lot of tires made it clear that the lateral G force while the vehicle is in the puddle is a function of the velocity that contains two parameters and that can be expressed by equation (10). This equation indicates the manner in which the ratio R of the lateral G force during cornering at a radius of 100R to the lateral G force when the vehicle enters the puddle changes according to the velocity u. (Refer to Figure 9.)

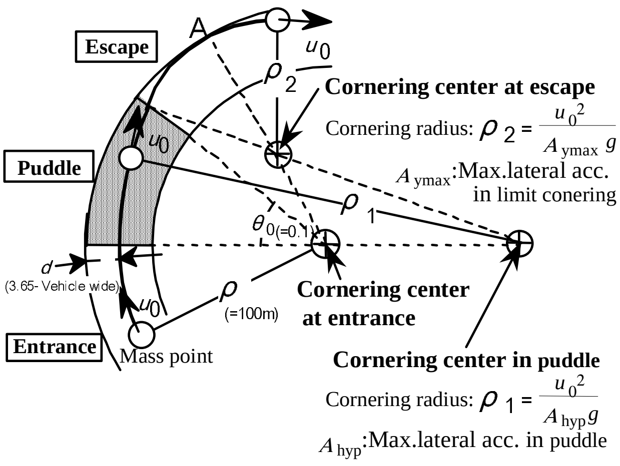


**Figure 8. The calculation of Hydroplaning in cornering**

$$R = \frac{1}{1 + e^{-grad(u - u_{offset})}} \qquad (10)$$

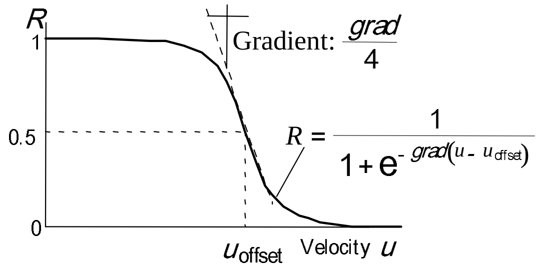


**Figure 9. The tire characteristics in the puddle**

Techniques were devised for using dynamic models to estimate the maximum entering velocity for the other courses as well.

## Verification of the accuracy of the estimation methods

Figures 10 and 11 show examples of the verification of the accuracy of the estimation methods described in sections of estimating method (with the horizontal axis representing the estimated values and the vertical axis representing the actual values). In each case, the accuracy is 3%-4%. The same level of accuracy was seen for the other courses as well, so the estimation methods are believed to be sufficiently accurate. The use of these techniques makes it possible to propose specifications at the design stage that will be satisfied with the target vehicle velocity, and it is believed that this would be useful for shortening the development period.

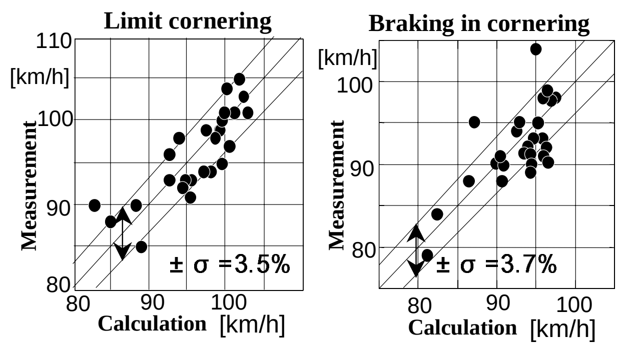


**Figure 10. The verification of calculation (1)**

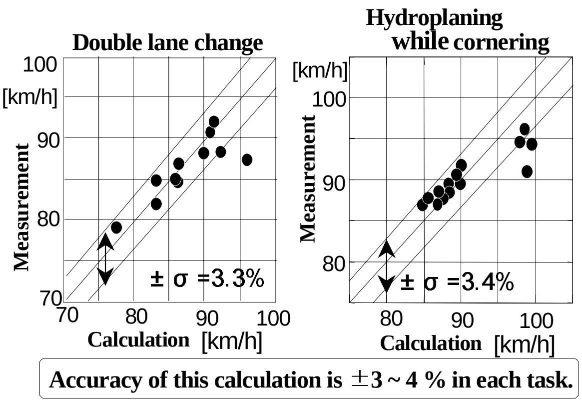


**Figure 11. The verification of calculation (2)**

### Influence of specifications

The influence of each specification of a given vehicle was calculated using the techniques described above, and the results are shown in Figure 12. From the graphs, it can be seen that in the case of a double lane change, the influence of the tires is smaller and the influence of the suspension specifications is greater than on other courses.

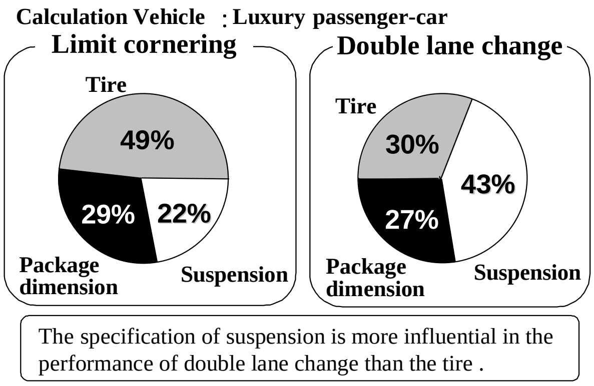


**Figure 12. The influence of specification**

### CONCLUSION

A method for estimating emergency handling was developed by excluding the influence of the basic specifications and comparing the suspension specifications and tire characteristics.

A method of estimating the maximum entering velocity for each course was also developed based on the basic specifications, the tire characteristics, and the suspension specifications. This made it possible to propose specifications at the design stage that will be satisfied with the established target vehicle velocity. It is thought that this would be useful for shortening the development period.

From now on, the issue will become how to create methods of evaluation and estimation for vehicle behaviors such as the ease of vehicle control at limits that can not be evaluated only by estimated vehicle control limit due to vehicle velocity (e.g., a sense of fishtailing during lane changes).

### REFERENCES

(1) Braess. OptimaleFahrzeugbewegung beim Fahrspurwechsel. Automobil-Industrie 2/73, S55/58
(2) Hideki Sakai. Theoretical Consideration of Relation of Rear-Wheel Skid to Steering Input. SAE paper 970378
(3) Masato Abe. Movement and Control of Automobiles. Sankaido Publishing Co., Ltd. 1992.